Optical second-harmonic spectra of Si(001) with H and Ge adatoms: First-principles theory and experiment

V. I. Gavrilenko
Rudolph Technologies Inc., Flanders, New Jersey 07836

R. Q. Wu
Department of Physics and Astronomy, California State University, Northridge, California 91330

M. C. Downer, J. G. Ekerdt, D. Lim, and P. Parkinson
Texas Materials Institute, University of Texas at Austin, Austin, Texas 78712

(Received 12 July 2000; revised manuscript received 12 January 2001; published 5 April 2001)

We present calculated second-harmonic-generation (SHG) spectra of the Si(001) surface based on a first-principles description of eigenvalues and eigenvectors using *ab initio* pseudopotentials. We also present SHG spectra for Ge-covered Si(001). The theoretical results explain all essential features of recent experimental SHG spectra of the Si(001)-(2×1) surface with low coverages of hydrogen and/or germanium, which alter the E_1 resonance in contrasting ways. The strong adatom specificity of the spectra results from redistribution of the adatom-related electronic states on the surface.

DOI: 10.1103/PhysRevB.63.165325 PACS number(s): 78.66.−w, 42.65.Ky, 73.20.−r

I. INTRODUCTION

The interaction of adatoms with semiconductor surfaces underlies key technological processes such as epitaxial film growth and etching, and is one of the most fundamental problems in surface science. Recently, surface-specific optical spectroscopies, such as second harmonic generation (SHG) (Refs. 1–4) and reflectance difference (anisotropy) spectroscopy (RDS/RAS) (Refs. 5–7) have been applied to numerous semiconductor-adatom systems because of their noninvasive nature, high sensitivity to submonolayer adsorption, and strong dependence of the spectroscopic response on the adatom species. Such features are useful for real-time, *in situ* monitoring of surface dynamical processes involving adsorbates.[8] On the other hand, microscopic explanation of the rich variety of adsorbate-specific spectroscopic responses through first-principles theory remains a challenge. Accurate spectroscopic SHG data on well-characterized surface-adsorbate systems[3,4,9–12] have become available only recently. The microscopic calculations have been compared with SHG spectra only for the Si(001):H system,[13] and have been limited to the semiempirical tight-binding method (SETBM).[13–15] Early SETBM calculations[14] predicted that adsorption of 1 ML hydrogen would remarkably modify the surface susceptibility $\chi^{(2)}_{zzz}(2\omega)$ of Si(111) and Si(001) surfaces in the spectral region $(1.5<2\hbar\omega<2.0$ eV) where surface states dominate, but would barely change it near E_1 (3.3–3.4 eV) and E_2 (4.2 eV), in contradiction to experiments.[3,4] A more recent SETBM study of Si(001) (Ref. 13) included all nonvanishing $\chi^{(2)}$ components into the SHG efficiency, $R_{pp}(2\omega)$, but still did not explain the strong effect of monohydride termination on the surface E_1 resonance.

In this paper, we present first-principles calculations of SHG spectra of Si(001)-adsorbate systems, and compare them to SHG experiments on clean and H-terminated Si(001),[4] and to new data for Ge-terminated Si(001), in the range $3.1<2\hbar\omega<3.5$ eV. This expanded database tests the theory more stringently than a single adsorbate, because H and Ge alter the SHG spectrum of clean Si(001)-2×1 in very different ways.

II. SURFACE SHG

Within its penetration depth beneath the surface, the incident light field at the frequency ω (E^{ω}) induces second-harmonic bulk (b) polarization densities of the form

$$P_i^{b,2\omega}=\chi^{(2)bd}_{ijk}E^{\omega}_j E^{\omega}_k+\chi^{(2)bnl}_{ijkl}E^{\omega}_j\nabla_k E^{\omega}_l\,. \tag{1}$$

In semiconductors and insulators, the nonlinear response originates from anharmonic bond polarizabilities. The leading bulk dipole term in Eq. (1) vanishes in centrosymmetric Si and Ge crystals. The second term, which is proportional to $\vec{\nabla}E$, is the electric quadrupole component.[16]

At a surface or interface, inversion symmetry is broken by (i) the structural discontinuity, including strain and chemical modifications unique to the surface/interface; and (ii) the discontinuity in the normal component of the electric field. Both discontinuities occur over a thickness of only a few atomic layers, and are thus sources of second-order nonlinearity. For macroscopic calculations, they are often combined into an effective surface dipole polarization density: $P_i^{s,2\omega}(\mathbf{r})=\chi^{(2)s,\mathrm{eff}}_{ijk}E^{\omega}_j(\mathbf{r})E^{\omega}_k(\mathbf{r})\delta(z)$, where $\delta(z)$ represents an infinitesimally thin radiating dipole sheet placed either just above or just below the surface.[17] Alternatively, the interface region can be approximated as a discrete thin film of finite thickness

d, to which a local nonlinear susceptibility $\chi_{ijk}^{(2)s,\mathrm{eff}}$, and linear dielectric constants with either bulk values or ''intermediate'' values unique to the surface region, are assigned.[18] In the latter case, the usual boundary conditions for continuous tangential electric and magnetic fields across the upper and lower interfaces must be applied in calculating harmonic fields.

Our treatment of boundary conditions for microscopic calculations of $P^{s,2\omega}$, as in other recent SHG calculations,[13,15] most closely resembles the latter approach. Specifically, the surface region is modeled as a slab of finite thickness (typically 8 to 10 ML). For electric fields in the slab, we use the external fields corrected by the relevant Fresnel factors. Spurious SHG from the back surface of the slab is suppressed by incorporating a smoothed step function $S(z)$ (equal to 1 at the front surface and 0 at the back surface) into the quantum-mechanical operators when evaluating matrix elements that contribute to $\chi_{ijk}^{(2)s}$.[13] The Fresnel coefficients are determined using dielectric functions calculated for bulk Si. For comparison with experiment, it is important to realize restrictions of the model used. The most important is the neglect of the electric field discontinuity and additional screening on the surface. This will result in errors of predicted absolute SHG intensities. These errors will be greatest for contributions to $\chi^{(2)s}$ that involve excitations of surface states, less for those related to the back bonds. In the present work, we are primarily interested in calculating *relative* SHG spectral intensities for different adsorbates, and spectral regions where back bond contributions dominate. For these cases, we find that the predicted SHG behavior agrees reasonably well with experiment.

Below we calculate this surface second-harmonic polarization for Si or Si/Ge slabs of 8–10 ML thickness. The functions of $\chi_{ijk}^{(2)}(-2\omega,\omega,\omega)$ are calculated in the independent particle picture, neglecting local field corrections and the nonlocality of the velocity operators in the polarization function.[19] In the length gauge $\chi_{ijk}^{(2)}(-2\omega,\omega,\omega)$ is given in atomic units ($e=1$, $\hbar=1$) by[20]

$$\chi_{ijk}^{(2)}(-2\omega,\omega,\omega)=\int \frac{d\mathbf{k}}{4\pi^3}[\chi_{II}^{ijk}(-2\omega,\omega,\omega)+\eta_{II}^{ijk}(-2\omega,\omega,\omega)+\sigma_{II}^{ijk}(-2\omega,\omega,\omega)], \tag{2}$$

$$\chi_{II}^{ijk}(-2\omega,\omega,\omega)=\sum_{nml}\frac{r^{i}_{nm}\{r^{j}_{ml}r^{k}_{ln}\}}{\omega_{ln}-\omega_{ml}}\times\left(\frac{2f_{nm}}{\omega_{mn}-2\omega}+\frac{f_{ml}}{\omega_{ml}-\omega}+\frac{f_{ln}}{\omega_{ln}-\omega}\right), \tag{3}$$

$$\eta_{II}^{ijk}(-2\omega,\omega,\omega)=\sum_{nml}\left[\omega_{nm}r^{i}_{nm}\{r^{j}_{ml}r^{k}_{ln}\}\times\left(\frac{f_{nl}}{\omega_{ln}^2(\omega_{ln}-\omega)}-\frac{f_{lm}}{\omega_{ml}^2(\omega_{ml}-\omega)}\right)+2\frac{f_{nm}r^{i}_{nm}\{r^{j}_{ml}r^{k}_{ln}\}(\omega_{ml}-\omega_{lm})}{\omega_{mn}^2(\omega_{mn}-2\omega)}\right]-8i\sum_{nm}\frac{f_{nm}r^{i}_{nm}\{\Delta^{j}_{mn}r^{k}_{mn}\}}{\omega_{mn}^2(\omega_{mn}-2\omega)}, \tag{4}$$

$$\sigma_{II}^{ijk}(-2\omega,\omega,\omega)=\sum_{nml}\frac{f_{nm}}{\omega_{mn}^2(\omega_{mn}-\omega)}\times[\omega_{nl}r^{i}_{lm}\{r^{j}_{mn}r^{k}_{nl}\}-\omega_{lm}r^{i}_{nl}\{r^{j}_{lm}r^{k}_{mn}\}]-i\sum_{nm}\frac{f_{nm}\Delta^{i}_{nm}\{r^{j}_{mn}r^{k}_{nm}\}}{\omega_{mn}^2(\omega_{mn}-\omega)}, \tag{5}$$

where $\Delta^{i}_{nm}\equiv p^{i}_{nn}-p^{i}_{mm}$, $\{r^{j}_{ml}r^{k}_{ln}\}\equiv\frac{1}{2}(r^{j}_{ml}r^{k}_{ln}+r^{k}_{ml}r^{j}_{ln})$, ω_{nm} is the energy difference between levels n and m, and $f_{nm}\equiv f_n-f_m$, with f_i the Fermi occupation factor for clean Si at zero temperature.[20] [The expression (5) is corrected for a factor $-i$ (Ref. 21) that was erroneously missed in Ref. 20.] Matrix elements $\mathbf{r}_{nm}$ were determined by $\mathbf{r}_{nm}=\mathbf{p}_{nm}/im\omega_{nm}$ through momentum matrix elements $\mathbf{p}_{nm}$,[20] which were calculated only in the upper half of the slab[15] to avoid contributions from the back surface. SHG reflectance efficiency R_{pp} was calculated using all nonvanishing $\chi^{(2)}$ tensor components.[13,15] Weak quadrupole contributions were not considered.

A. Numerical details

The surface structures were optimized by the Car-Parinello molecular-dynamics method based on density-functional theory (DFT) with *ab initio* pseudopotentials.[22] The electron-ion interaction was treated by norm-conserving, fully separable pseudopotentials in the Kleinman-Bylander form,[23] based on relativistic all-electron calculations for the free atoms by solving the Dirac equation self-consistently. Initially the pseudopotentials were generated by the Bachelet-Hamman-Schlütter (BHS) scheme[24] using the generalized gradient approximation (GGA) with exchange and correlation (XC) interaction as described in Ref. 25, and nonlinear core-valence XC as in Ref. 26. For structural relaxation, an energy cutoff up to $E_{\mathrm{cut}}=12$ Ry was used. Our calculated clean Si(001)(2×1) and Ge/Si(001) structures have asymmetric dimers with buckling of 0.76 Å, 0.79 Å (1 ML Ge), and 0.805 Å (2 ML Ge), respectively. Corresponding monohydride surfaces have symmetric dimers. These values agree well with previous findings,[7,27] but differ slightly from LDA values. For example, our GGA value of the bulk Si lattice constant slightly exceeds, and our LDA

value slightly underestimates, the experimental value. Surface atomic structures [e.g., dimer buckling 0.76 Å (GGA), 0.71 Å (LDA) (Ref. 28)] also differ slightly. For a given atomic structure, however, test calculations indicated that the SHG functions were insensitive to the method (GGA or LDA) of pseudopotential generation.[29,30]

Calculations of electronic-structure and optical properties were also based on the GGA.[22] Eigenvalues and wave functions were obtained by direct diagonalization of the Hamiltonian after full convergence of the self-consistent charge-density calculations, using the calculated equilibrium atomic structure as input. We modeled the surface by a slab of $N_{sl}=12$ ML, and used up to 48 **k** points ($N_{\mathbf{k}}$) in the irreducible 2D Brillouin zone (BZ), with $E_{\mathrm{cut}}=15$ Ry. Our GGA values of bulk Si optical transitions agree much better with experiment than our LDA values [e.g., $E_1=3.41$ eV (experiment), 3.1 eV (GGA), 2.75 eV (LDA)]. To match calculated optical transition energies to experimental values in fully *ab initio* calculations, one should use quasiparticle (QP) (e.g., GW) corrections. In the present calculations, quantum size effects in the surface slab further blueshift the conduction band by ~ 0.3 eV, shifting our calculated E_1-related SHG structure very close to the measured value (3.35 eV). Thus for these particular systems no further QP shifts were used.

B. SHG measurements

The SHG measurements were performed in an ultrahigh-vacuum (UHV) chamber with capabilities described previously.[4] Ge was deposited on Si(001) at 410 K using atomic layer epitaxy cycles with a gas mixture of 4% GeH_4 or Ge_2H_6, followed by H desorption. SH signals were generated by 90-fs fundamental pulses tunable from 1.5 to 1.75 eV in a p-in/p-out reflection configuration enabling $2\hbar\omega$ to be tuned through the Si E_1 resonance. Further experimental details are being reported separately.[11]

III. REFLECTANCE DIFFERENCE SPECTRUM

As a preliminary test, we calculated the well-studied[28,31–33] linear reflectance difference spectra (RDS) $\Delta R(\omega)/R=(\Delta R[110]-\Delta R[1\bar{1}0])/R_o$ (Ref. 33) of clean Si(001)(2×1) using 64 **k** points in the irreducible part of the BZ for the integration in reciprocal space. Our GGA result agrees reasonably well with experiments on single dimer Si(001)(2×1) surface,[32] as shown in Fig. 1. The overall magnitude of $\Delta R(\omega)/R$ agrees better than previous calculations,[28,31,33] and our calculated RDS peaks at 1.4, 2.6, and 2.9 correspond to measured peaks at 1.6 and 3.1 eV, which can be clearly identified as optical transitions between (2×1) dimer-related bonding and antibonding surface states.[28] In a previous LDA study of RDS on Si(001)(2×1),[33] we used the **k**-dependent QP corrections ($\Delta_{\mathbf{K}}$) calculated for bulk Si,[34] taking the corresponding data of the lowest conduction bands for $\Delta_{\mathbf{K}}$ values of the surface states. Despite differences at low frequencies attributable to this correction to the surface states, the overall agreement between the present GGA results, our previous LDA-QP data, and LDA-QP data of Refs. 31 and 28 (where scissorslike QP corrections were used) is very good.

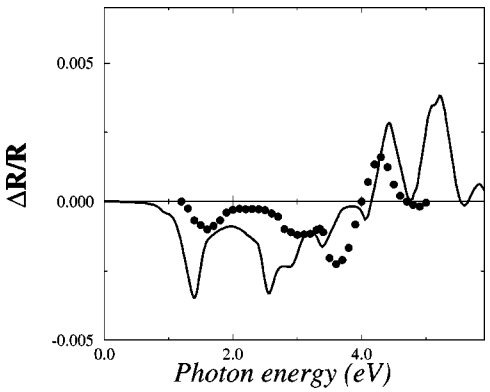

FIG. 1. Calculated RD spectrum (solid line) of clean single domain Si(001)(2×1) surface. Experimental RDS data of Ref. 32 are shown by dots.

IV. SHG RESULTS

In Figs. 2–6, the calculated spectra of five nonequivalent components of $\chi^{(2)}_{ijk}(-2\omega,\omega,\omega)$ for (2×1) geometry are shown for the spectral range between 0 and 6.0 eV. The y axis is oriented along $(1\bar{1}0)$ direction. The (xxz) and (zxx) components appear less intense, however the (zzz) component provides a strong contribution to the polarization on all the surfaces studied. Adsorption of Ge and/or H atoms results in quite complicated interplay between different components. The previous SETBM study of the SHG on

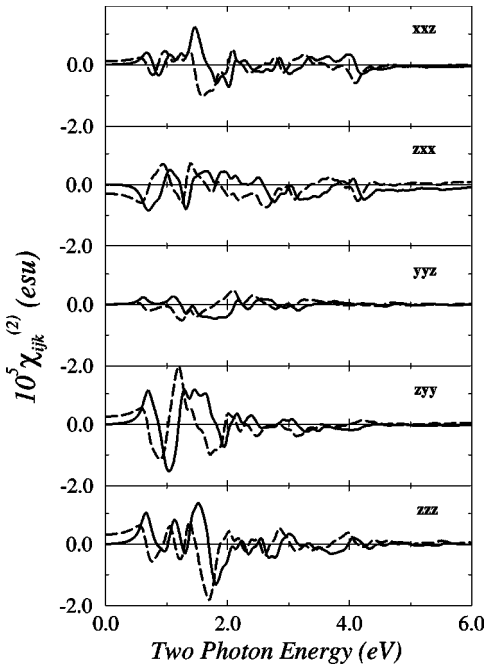

FIG. 2. Calculated nonequivalent components of the second-order optical susceptibility $\chi^{(2)}_{ijk}(-2\omega,\omega,\omega)$ of bare Si(001)(2×1) surface. The real and imaginary parts are shown by dashed and solid lines, respectively.

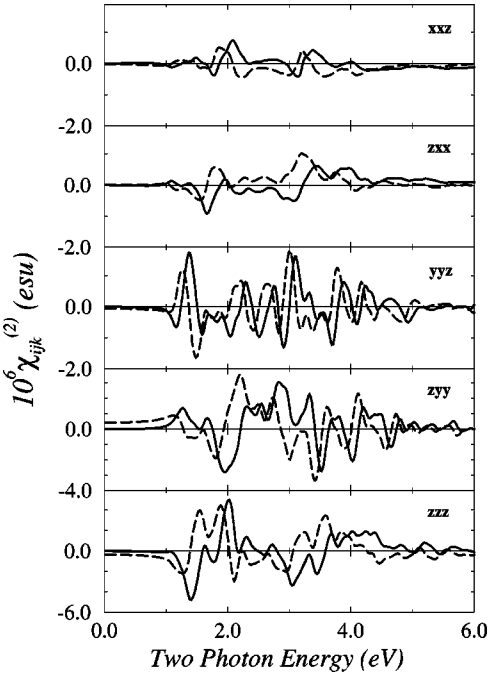

FIG. 3. The same as Fig. 2 but for monohydride Si(001)(2 $\times$1):H surface.

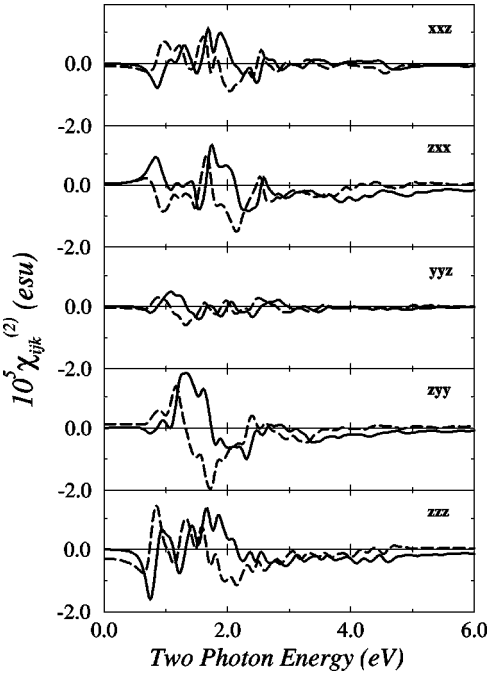

FIG. 5. The same as Fig. 2 but for Si(001)(2 $\times$1):Ge (2 ML) surface (with two monolayers of Ge).

Si(001)(2$\times$1) surface, however, reported the dominance of the $(yyz)+(xxz)$ components only.[13]

In Fig. 7(a), the calculated SHG spectra of clean Si(001)(2$\times$1) (solid curve) and monohydride Si(001)(2$\times$1):H (dashed curve), and the corresponding measured spectra (open and filled circles, respectively) are presented for $2.8<2\hbar\omega<3.7$ eV. For clean Si(001)(2 $\times$1), our calculations show a pronounced E_1 peak at 3.35 eV with shoulders at 3.24 and 3.06 eV, as also predicted by SETBM.[13] The 3.35- and 3.06-eV features agree well with observed features (the 3.24 eV feature is not resolved), as also pointed out by Mendoza *et al.*[13] Significantly, the present calculation quantitatively explains the strong quenching of these peaks by monohydride termination, which was not explained by SETBM.[13] It also reproduces the H-induced redshift of the E_1 feature, but overestimates its magnitude.

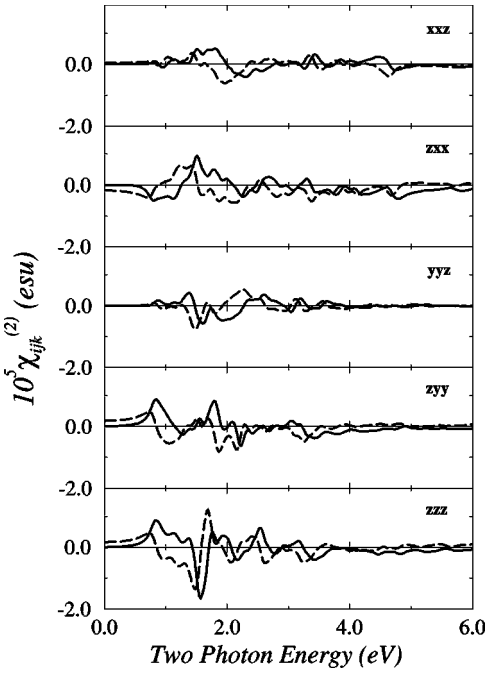

FIG. 4. The same as Fig. 2 but for Si(001)(2 $\times$1):Ge (1 ML) surface (with one monolayer of Ge).

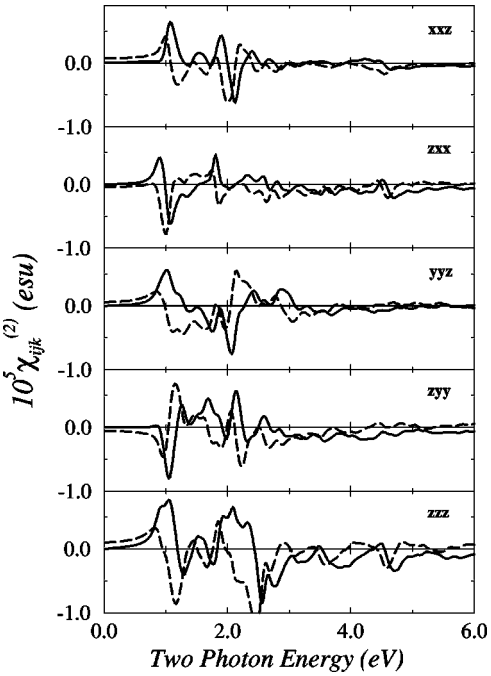

FIG. 6. The same as Fig. 2 but for monohydride Si(001)(2 $\times$1):Ge (2 ML):H surface (with two monolayers of Ge).

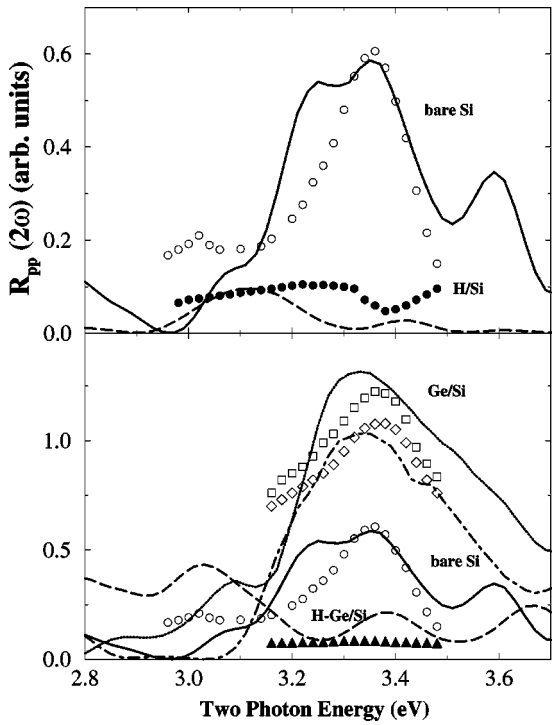

FIG. 7. Calculated and measured SHG efficiency spectra $R_{pp}(2\omega)$ near E_1 peak. (a) Clean Si(001)-(2×1): theory (solid curve), experiment (open circles); Si(001)-(2×1):H (1 ML), theory (dashed curve), experiment (filled circles). (b) Clean Si(001)-(2×1): theory (solid curve), experiment (open circles) as in (a); Si(001):Ge (1 ML), theory (dot-dashed curve), experiment (diamonds); Si(001):Ge (2 ML), theory (heavy dotted curve) and experiment (open squares); Si(001):Ge (2 ML) with saturation H coverage, theory (dashed curve), experiment (filled squares). Units for calculated R_{pp} are 10^{-18} W cm^{-2}.

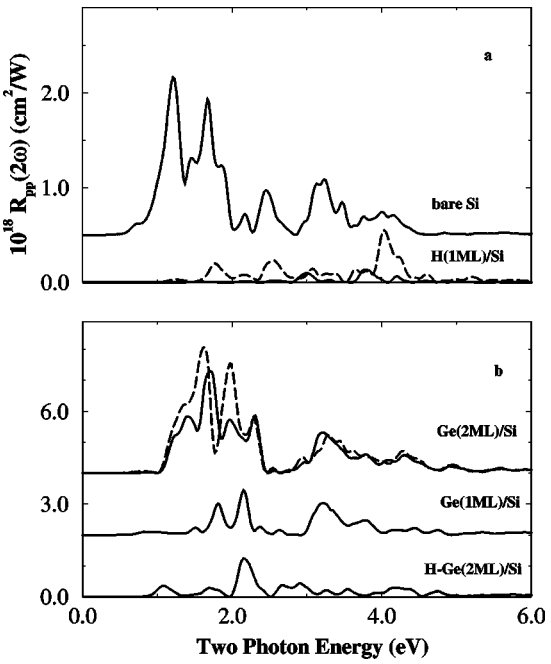

FIG. 8. Calculated SHG efficiency spectra $R_{pp}(2\omega)$ for extended spectral range. Curves have been displaced vertically for clearer viewing. (a) Clean Si(001)-(2×1) (upper solid curve), Si(001)-(2×1): H (1 ML) [fully relaxed structure (lower solid curve); structure held artificially to that of the clean Si(001)-(2×1) (dotted curve)]. Inset shows calculated equilibrium structures for clean Si(001)-(2×1) and Si(001)-(2×1):H surfaces viewed along [110]. (b) Clean Si(001)-(2×1), fully relaxed Si(001):Ge (1 ML), and Si(001):Ge (2 ML) (solid curves); Si(001):Ge (2 ML) with saturation H coverage (lower dotted curve); Si(001):Ge (2 ML) with buckling reduced artificially to 0.70 Å (upper dotted curve). Inset shows calculated structure for the Si(001):Ge (2 ML) surface.

This discrepancy may originate from increasing bulk quadrupole character as the surface dipole contribution weakens, evidenced by strong azimuthal anisotropy of SHG from H-Si(001).[35] The observed 3.25-eV peak is consistent with convolution of bulk (3.4 eV) and redshifted (3.15 eV) surface dipole E_1 features.

In Fig. 7(b), calculated SHG spectra for clean Si(001)(2×1) (solid curve), Si(001):Ge(1 ML) (dot-dashed), Si(001):Ge(2 ML) (dotted), and H-terminated Si(001):Ge(2 ML) (dashed), and corresponding measured spectra (open circles, diamonds, open and filled squares, respectively) are presented for the same spectral range. The calculated and observed spectra agree very well in basic trends: in contrast to H, adsorption of 1 (2) ML Ge *intensifies* the 3.35 eV peak threefold (fivefold) *without* spectral shift; subsequent H adsorption on the Ge-covered surface sharply quenches this feature. Agreement is best for Ge-induced trends, (where surface dipole contributions dominate) but it is poorest for the H-terminated surface, where quadrupole contributions are significant. Significant discrepancies in line shapes also remain. Nevertheless, the present theory reproduces the main observed *adsorbate-specific* trends of the SHG spectra.

Figure 8 presents calculated SHG spectra over the expanded range $0<2\hbar\omega<6$ eV for comparison with RDS and other linear optical spectra. Bare Si SHG peaks near 3.3 and 4 eV [Fig. 8(a)] are related to E_1 and E_2 bulk resonances, respectively, although their energies are significantly lower than the bulk Si values of $E_1=3.41$ eV and $E_2=4.3$ eV.[36] These features cannot arise directly from bulk bonds since SHG vanishes in the centrosymmetric bulk. However, their appearance in the SHG spectrum and the ''softening'' of their energies can both be explained by deformation of backbonds located near the surface, together with the strong localization of the SHG response at the surface. The more intense, lower-frequency ($2\hbar\omega\leqslant 3.0$ eV) peaks in Fig. 8(a) originate from surface states associated with dimers and dangling bonds. This assignment is supported by the calculated result that SHG peaks at 0.68, 1.2, 1.45, 1.7, and 1.85 eV are eliminated by monohydride adsorption [Fig. 8(a), lower solid curve], which symmetrizes and depolarizes the surface dimer and passivates dangling bonds, but strengthened and blue-shifted by Ge adsorption [Fig. 8(b), upper two solid curves], which increases the asymmetry and polarization of the dimer. This assignment is further supported by studies of the linear optics of the Si(001)(2×1) surface, which attribute RDS features in this spectral region to surface states.[37] Spe-

cifically, the cluster of peaks at 1.2, 1.45, and 1.7 eV, on the one hand, and the 2.6-eV SHG peak, on the other, share a common origin with RDS peaks at 1.4 and 2.6 eV, respectively, in Fig. 1. The low-frequency part of the predicted SHG spectra, however, should be considered cautionary by comparison with experiment. As it has been pointed out above, the reason for this is neglect of the discontinuity of the electric field normal component and additional screening on the surface. These points should be addressed in the future SHG studies.

Convergence of RDS and SHG spectra with respect to $E_{\rm cut}$, number of empty electron states, N_{sl}, and $N_{\mathbf{k}}$ was carefully analyzed. Neither RDS nor SHG changed remarkably for $E_{\rm cut} \geqslant 15$ Ry, nor by including empty states with energy $\geqslant 1$ Ry. On the other hand, our SHG spectra converged very well with $N_{\rm sl}=8$, while the low-frequency ($\hbar\omega \leqslant 3$ eV) RDS converged within 10–15% only for $N_{\rm sl} \geqslant 12$. Higher-frequency RDS peaks at 4.3 and 5.3 eV continued to change significantly with increasing $N_{\rm sl}$. Previous RDS calculations of Si(001)(2×1) with $N_{\rm sl}=16$ (Ref. 31) and $N_{\rm sl}=32$ (Ref. 33) confirm these trends. The faster convergence of SHG with $N_{\rm sl}$ stems from its stronger surface localization in covalent cubic materials. Finally, convergence of RDS and SHG spectra was checked for $N_{\mathbf{k}} \leqslant 96$. In the region of present experiments (2.8 eV $\leqslant 2\hbar\omega \leqslant$3.7 eV), the SHG spectrum with $N_{\mathbf{k}}=48$ converged within 15–20 %, a reasonable compromise in view of computational complexity. Analysis of low-frequency spectra, and representation of line shapes, however, should improve with higher $N_{\mathbf{k}}$ in future computations.

Compared to SETB calculations, our SHG spectra were relatively insensitive to small deviations from calculated equilibrium structure. For example, the calculated spectrum of a surface with the atomic structure of clean Si(001)(2×1) but with H-saturated dangling bonds [Fig. 8(a), dashed curve] shows a greatly weakened SHG response, qualitatively similar to that of fully relaxed Si(001) $\times(2\times1)$:H. As a second example, the calculated spectrum of Ge (2 ML)/Si(001) with dimer buckling reduced artificially to 0.700 Å [Fig. 8(b), upper dashed curve], particularly near 3.35 eV [Fig. 2(b), light dotted curve], does not differ greatly from that of the fully relaxed surface. Such calculations demonstrate that adsorbates change surface SHG spectra primarily by altering surface chemical bonds, rather than by altering surface atomic structure.

An important remaining question is the underlying reason for the strong sensitivity of the ''bulklike'' 3.3-eV peak to monohydride and Ge surface adsorption. In light of the origin of this feature in deformed backbonds, it is tempting to attribute this sensitivity to adsorbate-induced structural changes in the backbond region. For example, symmetrization of the surface dimer by monohydride termination slightly alters atomic positions in lower layers, which might quench the E_1 SHG intensity. Moreover Ge termination induces a tensile strain gradient in the Si backbonds because of the 4% mismatch in lattice constant between Ge and Si, which could conceivably enhance the E_1 SHG intensity. However, such ''structural'' explanations are inconsistent with experimental trends. The change in backbond structure induced by mono-H termination is slight compared to the massive strain relief induced by dimer-breaking dihydride termination, yet the former affects the observed SHG E_1 intensity more strongly. Moreover, hydrogen termination of the Ge-covered Si surface barely affects the lattice mismatch strain, yet it completely quenches the SHG E_1 intensity.

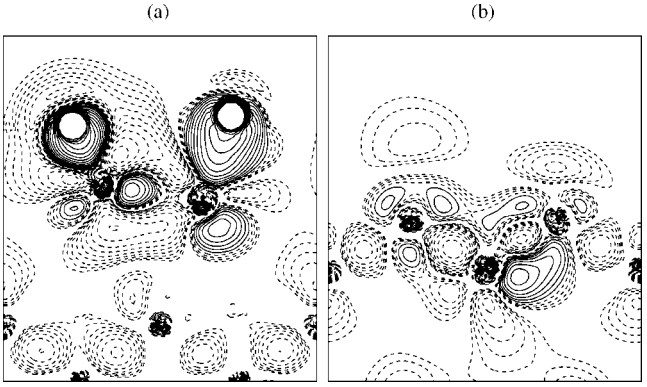

FIG. 9. Calculated valence charge-density differences between bare and unrelaxed monohydride Si(001)(2×1) surfaces, $\rho_{\rm bare} - \rho_{\rm mono}$. The charge maps are cut through the vertical $[\bar{1}10]$ planes located at $Y=0$ [panel (a)] and at $Y=a_y$ [panel (b)] in the unit cell. Contours start from $\pm 1\times10^{-3}$ e/a.u.^{3} and increase successively by a factor of $\sqrt{2}$. Dashed (solid) lines indicate charge accumulation (depletion) in the electron density.

A more consistent explanation is that adsorbates ''chemically'' influence underlying bonds via orbital rehybridization, or charge transfer. In fact, the intensity of the E_1 peak, despite its backbond origin, is closely correlated with the dimer asymmetry, which in turn is accompanied by a strong charge transfer to the uppermost Si atom from underlying layers. In order to quantify this charge transfer, we calculated charge distribution maps of bare and monohydride Si(001)(2×1) surfaces. In Fig. 9, the charge differences, $\rho_{\rm bare}-\rho_{\rm mono}$, between these two surfaces are presented. [In order to demonstrate only ''chemical'' mechanisms of the charge transfer due to the H adsorption on the Si(001)(2×1) surfaces, the $\rho_{\rm mono}$ is calculated for an unrelaxed (unsymmetrized) dimer structure.] The 2D charge maps are cut through the two vertical $[\bar{1}10]$ planes located at $Y=0$ [Fig. 9(a)] and at $Y=a_y$ [Fig. 9(b)] in the unit cell. Adsorption of hydrogen causes strong charge redistribution in the atomic bonds of the few topmost layers. The strong effect of H on the E_1 peak can thus be attributed to charge transfer between the immediate subsurface backbonds and the adsorbate atom. Stated equivalently, the sensitivity of the E_1 peak to H results from strong hybridization of Si and H orbitals in the backbond region. This explains the failure of SETB calculations based solely on Si sp^3s^* orbitals—i.e., without explicit inclusion of H orbitals—to predict the strong affect of monohydride on the E_1 peak.

Similar conclusions regarding the dominance of ''chemical'' over ''structural'' mechanisms have been reached independently in two other recent SHG studies of adsorbate interactions with silicon surfaces. Lim *et al.*[12] found that incorporation of boron at second-layer substitutional sites of Si(001) strongly affected the SHG E_1 feature. Even though

second-layer boron substantially reconstructs the surface, the SHG changes were explained predominantly in terms of charge transfer from the surface Si atoms to the underlying boron acceptors. In fact, the principal trends were satisfactorily reproduced by models that neglected the adsorbate-induced structural change. In this case, H termination of the boron-reconstructed surface *enhanced* the E_1 intensity, because the strong boron acceptors then preferentially drew charge from underlying Si atoms. Mitchell *et al.*[38] studied the rotational anisotropy of SHG in reflection from Si(111) surfaces with covalently attached monolayers of -H, $-C_{10}H_{21}$ (decyl), -Cl, $-O-C_{10}H_{21}$ (decyloxy), and with a native oxide film. The results showed that the dominant contributing component of the surface $\vec{\chi}^{(2)}$ increased in direct proportion to the electronegativity of the surface species. The latter was characterized by measurements of chemical shifts in Si $2p$ core-level photoelectron spectra, which have been shown to provide a useful measure of the polarization of the Si-Si backbonds by the electronegativity perturbation of the surface covalent bonds. The correlation between SHG and core-level shifts suggested that electronegativity perturbation is more important than strain in determining the SHG response. This conclusion was corroborated by results with organic overlayers, which yielded a relatively higher surface susceptibility despite their nonrigid, strain-free structure.

V. CONCLUSION

In conclusion, we present calculated second-harmonic spectra of Si(001) and its interaction with H and Ge adsorbates. Our results explain the strongly contrasting SHG response of Si(001) to H and Ge adatoms observed near the E_1 optical transition, and predict new adsorbate-specific SHG spectroscopy near-infrared surface-state resonances. Moreover, the calculations elucidate the strong sensitivity of the surface $\chi^{(2)}$ to chemical hybridization of surface adatom and substrate atomic orbitals, and provide a basis for improved calculations of both linear and nonlinear spectra of a wide range of surface-adatom systems.

ACKNOWLEDGMENTS

This work was supported by the U.S. Department of Energy (Grant No. DE-FG03-99ER14948), the computing grant at NERSC, the NSF Science and Technology Center Program (Grant No. CHE-8920120), the Robert Welch Foundation (Grant No. F-1038), the Air Force Office of Scientific Research (Contract No. F49620-95-1-0475), and the Texas Advanced Technology/Research Program (Grants No. ATPD-178 and No. ARP-0310-1999).

[1] J. R. Power, J. D. O'Mahony, S. Chandola, and J. F. McGilp, Phys. Rev. Lett. **75**, 1138 (1995).
[2] C. Meyer, G. Lüpke, U. Emmerichs, F. Wolter, H. Kurz, C. H. Bjorkman, and G. Lucovsky, Phys. Rev. Lett. **74**, 3001 (1995).
[3] U. Höfer, Appl. Phys. A: Mater. Sci. Process. **63**, 533 (1996).
[4] J. I. Dadap, Z. Xu, X. F. Hu, M. C. Downer, N. M. Russell, J. G. Ekerdt, and O. A. Aktsipetrov, Phys. Rev. B **56**, 13 367 (1997). SHG spectra for clean and H-Si(001) presented here are new data acquired with somewhat improved vacuum and surface cleanliness.
[5] T. Yasuda *et al.*, Phys. Rev. Lett. **74**, 3431 (1995); L. Kipp *et al.*, *ibid.* **76**, 2810 (1996); N. Esser *et al.*, *ibid.* **77**, 4402 (1996).
[6] C. Noguez, C. Beitia, W. Preyss, A. I. Shkrebtii, M. Roy, Y. Borensztein, and R. Del Sole, Phys. Rev. Lett. **76**, 4923 (1996).
[7] J. R. Power, P. Weightman, S. Bose, A. I. Shkrebtii, and R. Del Sole, Phys. Rev. Lett. **80**, 3133 (1998).
[8] P. Bratu and U. Höfer, Phys. Rev. Lett. **74**, 1625 (1995); C. E. Allen, R. Ditchfield, and E. G. Seebauer, J. Vac. Sci. Technol. A **14**, 22 (1996); S. Haraichi *et al.*, Jpn. J. Appl. Phys., Part 1 **35**, 2416 (1996); P. Kratzer *et al.*, Phys. Rev. Lett. **81**, 5596 (1998).
[9] W. Daum, H. J. Krause, U. Reichel, and H. Ibach, Phys. Rev. Lett. **71**, 1234 (1993).
[10] S. Chandola, M. Cavanaugh, J. R. Power, and J. F. McGilp, Thin Solid Films **313-314**, 565 (1998); J. R. Power, S. Chandola, J. D. O'Mahony, P. Weightman, and J. F. McGilp, Surf. Sci. **352-354**, 337 (1996).
[11] P. Parkinson, D. Lim, R. Büngener, J. G. Ekerdt, and M. C. Downer, Appl. Phys. B: Lasers Opt. **68**, 641 (1999)
[12] D. Lim, M. C. Downer, J. G. Ekerdt, N. Arzate, B. S. Mendoza, V. I. Gavrilenko, and R. Q. Wu, Phys. Rev. Lett. **84**, 3406 (2000).
[13] B. Mendoza, A. Gaggiotti, and R. Del Sole, Phys. Rev. Lett. **81**, 3781 (1998).
[14] V. I. Gavrilenko and F. Rebentrost, Appl. Phys. A: Mater. Sci. Process. **60**, 143 (1995); Surf. Sci. **331-333**, 1355 (1995).
[15] L. Reining, R. Del Sole, M. Cini, and J. G. Ping, Phys. Rev. B **50**, 8411 (1994).
[16] Y. R. Shen, *The Principles of Nonlinear Optics* (Wiley, New York, 1984).
[17] J. E. Sipe, J. Opt. Soc. Am. B **4**, 481 (1987).
[18] N. Bloembergen and P. Pershan, Phys. Rev. **128**, 606 (1962).
[19] V. I. Gavrilenko and F. Bechstedt, Phys. Rev. B **55**, 4343 (1997).
[20] J. L. P. Hughes and J. E. Sipe, Phys. Rev. B **53**, 10 751 (1996).
[21] J. L. P. Hughes (private communication).
[22] R. Stumpf and M. Scheffler, Comput. Phys. Commun. **79**, 447 (1994).
[23] L. Kleinman and D. M. Bylander, Phys. Rev. Lett. **48**, 1425 (1982).
[24] G. B. Bachelet, D. R. Hamman, and M. Schlütter, Phys. Rev. B **26**, 4199 (1982).
[25] J. P. Perdew, K. Burke, and M. Ernzerhof, Phys. Rev. B **54**, 16 533 (1996); Phys. Rev. Lett. **77**, 3865 (1996).
[26] M. Fuchs and M. Scheffler, Comput. Phys. Commun. **119**, 67 (1999).
[27] A. I. Shkrebtii (private communication); J. E. Sipe *et al.*, Phys. Status Solidi A **170**, 431 (1998).
[28] M. Palummo, G. Onida, R. Del Sole, and B. S. Mendoza, Phys. Rev. B **60**, 2522 (1999).
[29] C. Aversa and J. E. Sipe, Phys. Rev. B **52**, 14 636 (1995).

[30] V. I. Gavrilenko and R. Q. Wu, Phys. Rev. B **61**, 2632 (2000).
[31] L. Kipp *et al.*, Phys. Rev. Lett. **76**, 2810 (1996).
[32] R. Shioda and J. van der Weide, Phys. Rev. B **57**, R6823 (1998).
[33] V. I. Gavrilenko and F. H. Pollak, Phys. Rev. B **58**, 12 964 (1998).
[34] G. Cappellini, R. Del Sole, L. Reining, and F. Bechstedt, Phys. Rev. B **47**, 9892 (1993).
[35] Z. Xu *et al.*, J. Vac. Sci. Technol. B **15**, 1059 (1997).
[36] *Handbook of Optical Constants of Solids*, edited by E. D. Palik (Academic Press, London, 1985).
[37] R. Del Sole, in *Photonic Probes of Surfaces*, edied by P. Halevi (Elsevier, Amsterdam, 1995), p. 131.
[38] S. A. Mitchell, M. Mehendale, D. Villeneuve, and R. Boukherroub, Chem. Phys. Lett. (to be published).